The Effect of Boundary Conditions on Transient Airflow Patterns: A Numerical Investigation of Door Operation

Arup Bhattacharya
Student Member ASHRAE

Ehsan Mousavi, PhD
Associate Member ASHRAE

ABSTRACT

The characteristics of indoor airflow contributes to the dispersion patterns of contamination, and consequently, the quality of indoor air. To control contaminant dissipation, the understanding of airflow traits is of utmost importance. Boundary conditions in the indoor environment, such as a moving fluid-solid interface, can significantly change the airflow patterns. For example, in any indoor setting, doors are operated randomly and to accurately model the airflow, it is key to learn the transient effects of door opening and closing. But study transient airflow is very expensive and time consuming.

In this paper, computational fluid dynamics (CFD) models were developed to simulate the movement of a single hinged door separating two zones. Subsequent models, with the boundaries moved away from the door such that the zones had a larger area with the door being at a fixed location, were created and location-specific air velocity profile over the zone was measured. The main aim is to study the change in airflow patterns with respect to the wall location. Results showed that no-slip wall boundary conditions created a velocity gradient, and consequently, altered the original flow of air. For walls that are closer to the door, the velocity gradient was more significant. Knowing these patterns and potential correlations between them may enable the construction of a prediction scheme to approximate transient airflow patterns by a set of known models. We characterize the accuracy of the approximation models and compare the computational intensity to the traditional time dependent CFD approach.

INTRODUCTION

Indoor air is the most dominant exposure for humans, as more than 50 % of the total air intake in a lifetime is inhaled indoor. Thus, it is safe to assume that a large proportion of airborne illnesses stems from indoor air. Apart from the normal indoor environment, there are controlled indoor environment, (e.g. clean rooms, healthcare facilities) where the indoor air quality is of utmost importance. Given that industrial and pharmaceutical clean rooms are production environments, unpredictable airborne contamination can result in adverse undesirable consequences. Sensitive healthcare spaces, such as operating rooms, separation rooms, etc., should follow stringent restrictions in terms of air quality, as patients with open wounds and suppressed immune system are much more susceptible to airborne infection. In the United States alone, hospital acquired infections pose an estimated economic burden of $28-$45 billion per year (Stone 2009). Hence, maintaining a high degree of cleanliness requires the ability to predict the spread of airborne particles in the room (Rouaud and Havet 2002). And to that end, knowledge of the airflow characteristics is vital.

There are several factors affecting the patterns of air movement in spaces enclosed by boundaries. For example, existing literature suggests door motion is an important contributor to the characteristics of indoor airflow. A number of studies have shown how door opening has resulted in breakdown of isolation conditions, disrupting differential pressure and causing turbulence (Smith et al. 2013; Tang et al. 2005). Mousavi et al. showed that higher door speeds create turbulence

Arup Bhattacharya is a PhD Student in Construction Science and Management department, Clemson University, SC, USA (email: arupb@clemson.edu)

Ehsan Mousavi is an Assistant Professor in Construction Science and Management department, Clemson University, SC, USA (email: mousavi@clemson.edu)

and lead to change in airflow parameters, aiding in volumetric exchange under pressurized conditions (Mousavi and Grosskopf 2016). Gustavsson's study demonstrated that door opening was followed by creation of vortices and mixture of air from another space into confined operating room (Gustavsson N. 2010).

An indoor space is determined by the position and type of the boundaries. Boundaries act as barriers - hindering the free movement of air. An indoor space with narrow boundaries does not have plenty of space for the air to move freely, rather, the airflow velocity is zero at the wall (if no-slip condition is assumed), which generates turbulence when air strikes the wall at high velocity (Sekhar and Willem 2004). As a result, the changes in airflow characteristics are rapid in these spaces whereas spaces where boundaries are located far from each other provide sufficient area for the air to move without interference from the stationary walls. Thus, for a space with boundaries at a smaller distance from one another, the resulting flow pattern from door opening and closing will be different compared to a room with wider boundaries.

Most of the studies that have been carried out to investigate the effects of door opening did not consider the effect of room boundaries. Very little has been done to examine the combined effects of space boundaries and door movement on indoor airflow. This study aims to compare and scrutinize certain properties of the indoor air movement in environments where the spaces are defined by different boundary positions. Hence, a series of computational fluid dynamics (CFD) models was developed to simulate airflow patterns under different door opening and boundary conditions scenarios.

METHOD

Mathematical Model

CFD is a numerical technique to solve fundamental conservation equations for the flow field. With specific boundary conditions, the fluid flow patterns are determined by solving the continuity equation (Eq. 1) the conservation of momentum (Eq. 2) and energy (Eq. 3) equations.

$$\frac{\delta t}{\delta \rho} + \frac{\delta}{\delta x_i}(\rho u_i) = 0 \qquad \text{Equation – 1}$$

where ρ density of the fluid, u_i – velocity vector component (u, v and w), t represents time and x_i – Cartesian co-ordinate axis of x, y and z representing space.

$$\frac{\delta}{\delta t}(\rho u_i) + \frac{\delta}{\delta x_j}(\rho u_i u_j) = -\frac{\delta p}{\delta x_i} + \frac{\delta}{\delta x_j}[\mu(\frac{\delta u_i}{\delta x_j} + \frac{\delta u_j}{\delta x_i})] + \rho g_i \qquad \text{Equation – 2}$$

where, p - pressure, μ - kinematic viscosity and g_i - gravitational acceleration acting on the fluid elements in x, y and z direction.

$$\frac{\delta}{\delta t}(\rho H) + \frac{\delta}{\delta x_i}(\rho u_i H) = \frac{\delta}{\delta x_i}[\frac{k}{c_p}\frac{\delta H}{\delta x_i}] + S_H \qquad \text{Equation – 3}$$

where, where H - enthalpy, k - thermal conductivity of fluid element, c_p - specific heat and S - a source term.

The above equations are used to model viscous flows with transport phenomena of friction, thermal conduction and mass diffusion. More references on discussion regarding solution approach of CFD models can be obtained from (J Tu, GH Yeoh 2018)

The Reynold Averaged Navier-Stoke's method (RANS) is then applied to model turbulent flows, averaging the flow equations over much larger time scale than the turbulent motion. Out of many turbulence models developed by RANS, the two-equation RNG k-ε model is recommended for airflow in enclosed spaces (Chen 1995).

Simulation Model

Four different two-dimensional models (Figure 1) were prepared to simulate a hinged door opening and closing. For all the models, the door dimensions were fixed, and it was located at the center of the space.

The positions of the room walls varied in those models (Table 1) so that the room surface areas were different. A reference model was also prepared such that the room walls were sufficiently far from the door moving zone and those boundaries did not have interference with the free movement of air due to door motion (Table 1). The velocity magnitude and the gradients were recorded and compared between the models as well as between each model and the reference model.

Table 1. Dimension of Different Models

Model No.	Model Width - L1 in meter (feet)	Wall width - L2 in meter (feet)
Model – 1	2 (6.56)	0.49 (1.61)
Model – 2	3 (9.84)	0.99 (3.25)
Model – 3	4 (13.12)	1.49 (4.89)
Model – 4	5 (16.40)	1.99 (6.53)
Reference Model	10 (32.81)	4.49 (14.73)

ANSYS - 19.2 academic version was used for the CFD simulations. The RNG k-ε two equation with standard wall function was used to model turbulence. All the models were discretized using uniform meshing scheme and triangular meshing element. Mesh refinement processes continued to ensure the grid independence of surface-averaged velocity across the models and the number of cells after this process for each model is tabulated in Table 2. The simulations were considered to be isothermal as no heat sources were considered.

Table 2. Post-mesh Cell Information

Model No.	No. of Cells	Max. Aspect Ratio	No. of nodes per Sq. meter
Model – 1	24813	7.85491e+00	2250
Model – 2	27120	7.46292e+00	2016
Model – 3	42460	6.94546e+00	1925
Model – 4	55672	7.02621e+00	2019
Reference Model	112756	7.29450e+00	2053

Three different boundary conditions were used - room walls, doorwall and pressure outlets (Figure1). All the walls were considered to be stationary with no-slip condition - where velocity components in both x and y directions were zero. The door was hinged as shown in Figure 1. A user defined profile prescribed the opening-closure cycle such that it took two seconds for the door to fully open, stayed at rest for one second and then closed fully in another two seconds. This cycle was the average door opening cycle for operating rooms reported in the literature.

The angular frequency ω was set in a way such that at time 0, the door was closed ($\omega = 0$), after 1 second - the door was half open ($\omega = \pi/2$), after 2 seconds - the door was fully open ($\omega = 0$) and remained ajar for 1 second. At second 3, the door started closing. After 4 seconds - the door was half closed ($\omega = \pi/2$) and at second 5 - it was fully closed ($\omega = 0$).

The simulations were performed for 20 seconds with a fixed time step size of 0.01 seconds (2000-time steps) for all models apart from model 1, where the time step size was 0.008 seconds (2500 time steps) in order to avoid negative cell volume during the transient simulation. The convergence criteria on normalized residuals was set to 10^{-4}.

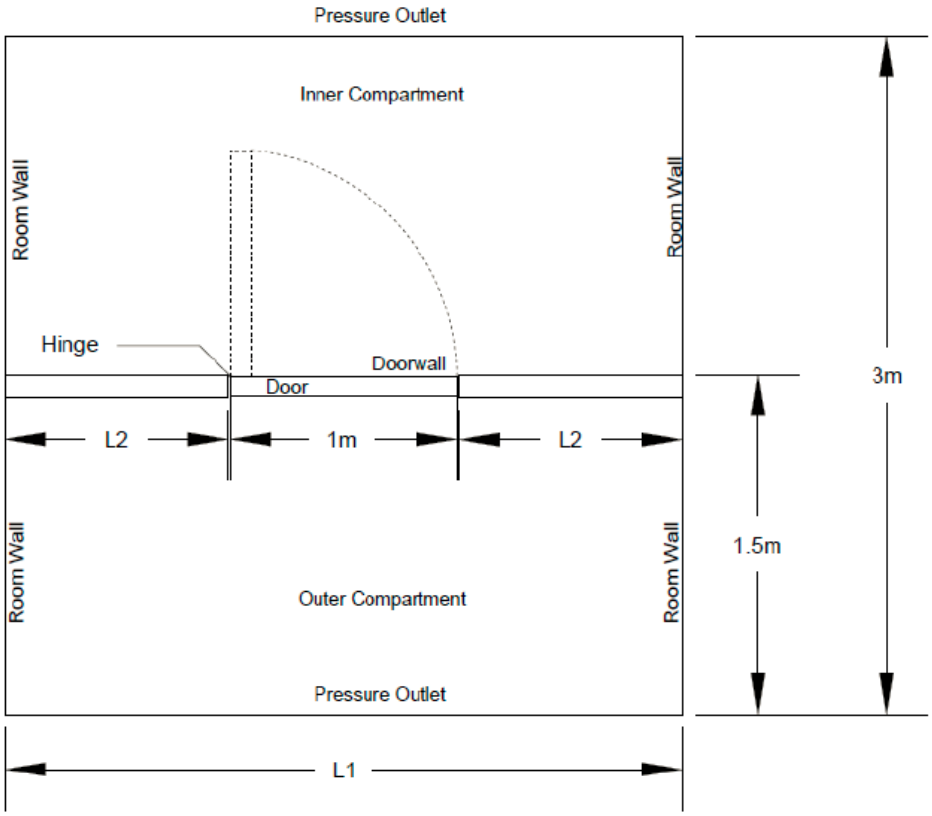

Figure 1. Simulation Model

Next, the results obtained from the simulations were processed. Once a CFD solver solves the problem over the discretized region, a solution is obtained at every node. Now, given that after meshing the nodes generated for each model were located at different coordinates, the obtained results were also available at discrete points for all the models. In order to be able to compare the models, the properties had to be available at common locations over all the region. This was achieved by interpolation - the simulation results spread over discrete points were distributed evenly in grids which were sized in coherence with the original model's length to width ratio; i.e. for all the models, the x-axis of the grids had equal distribution points - 60 and the y-axis of the grids had different distribution points, which increased as the width of the models increased (Table 3).

To facilitate effective analysis of comparative results for models with different surface areas, shared regions were defined. A shared region was a region of same grid size for two different models but as grid widths were different, for the wider model, the width was truncated to suit that of the narrower model in comparison so that both these models had same grid size. After truncation, only the velocities at these imposed boundaries were assumed to be null without altering any other result.

RESULTS AND DISCUSSION

Velocity Distribution

The velocity magnitudes across the shared region followed similar trends. Figure 2 describes the contours of velocity for Model-1 at time 1s, 2s, 3s, 4s, 5s, and 10s. The airflow speed due to door movement was greater during the closing period compared to the opening period. While the door was moving, the highest velocity was always at the region closest the tip of the outer door surface, a point which travels the largest distance during the transient door movement. When

the door was half-open while opening, the maximum velocity magnitude reached 1.8 m/s (5.91 ft/s) and reduced below 1 m/s (3.28 ft/s) when the door was fully open.

Table 3. Grid Size of Interpolated Data

Model No.	Grid Size
Model – 1	60 x 40
Model – 2	60 x 60
Model – 3	60 x 80
Model – 4	60 x 100
Reference Model	60 x 199

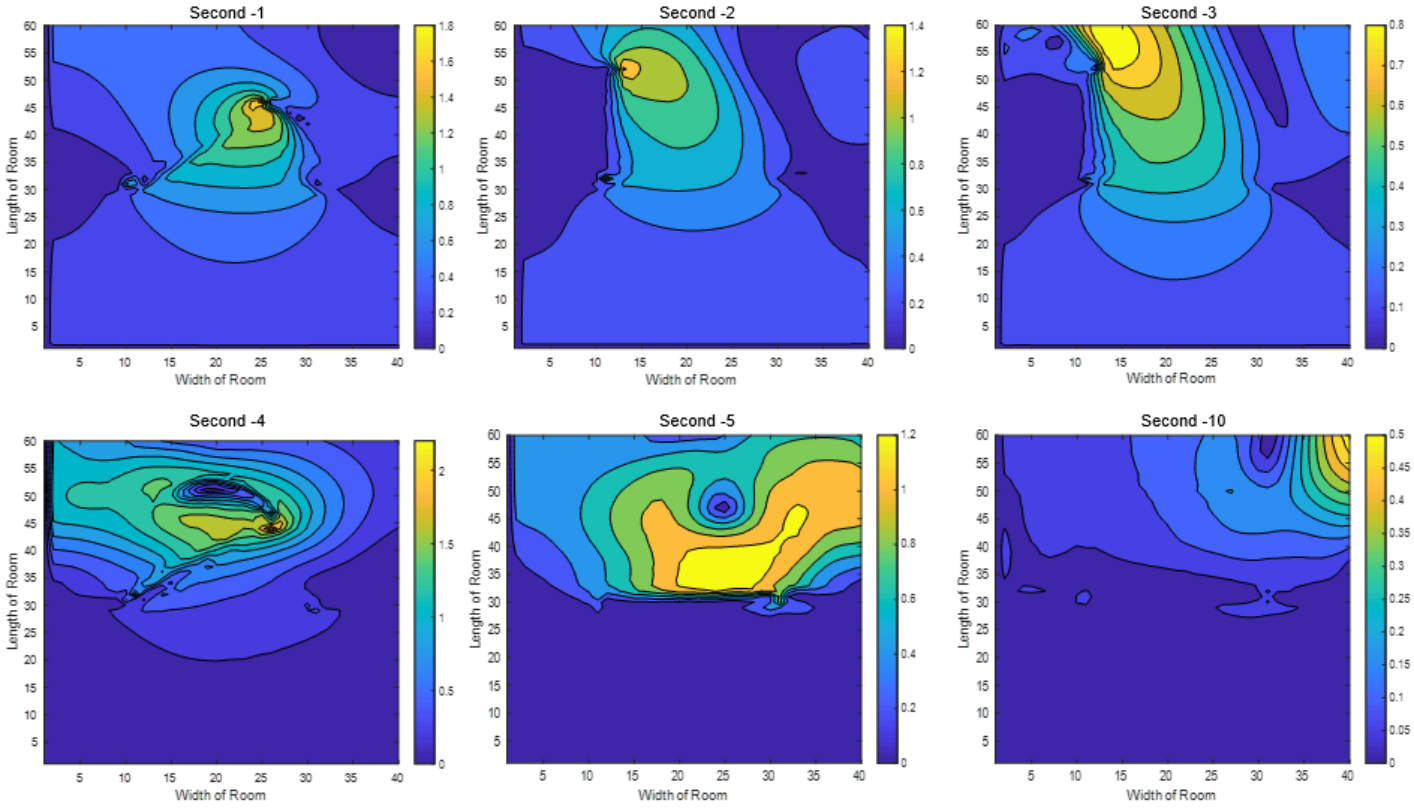

Figure 2. Velocity Distribution at Different Times for Model – 1

During the closing cycle of the door, the velocity reached a maximum value of greater than 2 m/s (6.56 ft/s) in a small region around the tip of the door. In second five, the door was fully closed, the magnitude of the velocity dropped down to a maximum of 1.2 m/s (3.94 ft/s). Higher velocities during the closing cycle was due to the residual velocities. During the opening of the door, the air in the space was still. But during the closing cycle, there was air movement and the streamlines were following the direction obtained from opening motion. The initial condition when the door was closing was different than when the door was opening. This difference created vortices which caused the velocity to increase in magnitude. After the door was closed, the air streamlines moved away in the direction that was created by the door closing motion. Five seconds after the door was closed, the maximum velocity was found near the right wall with a magnitude of close to 0.5 m/s (1.64 ft/s). Approximately 12 seconds after door closure, the maximum velocity at any point of the region dropped below 0.15 m/s (0.49 ft/s), i.e. there was no air movement anymore.

Comparison of Maximum Velocities in Different Models

The largest magnitude of velocity was found consistently at the tip of the door when the door was half-open during the closing cycle. The point x=1.0m (3.28 feet), y=0s and t=*4*s in time and space (coordinates are from the hinge) was used to illustrate velocity magnitude along the x- and y- axes (Figure 3). As the boundaries were pushed farther, the contours were confined and did not reach the boundaries.

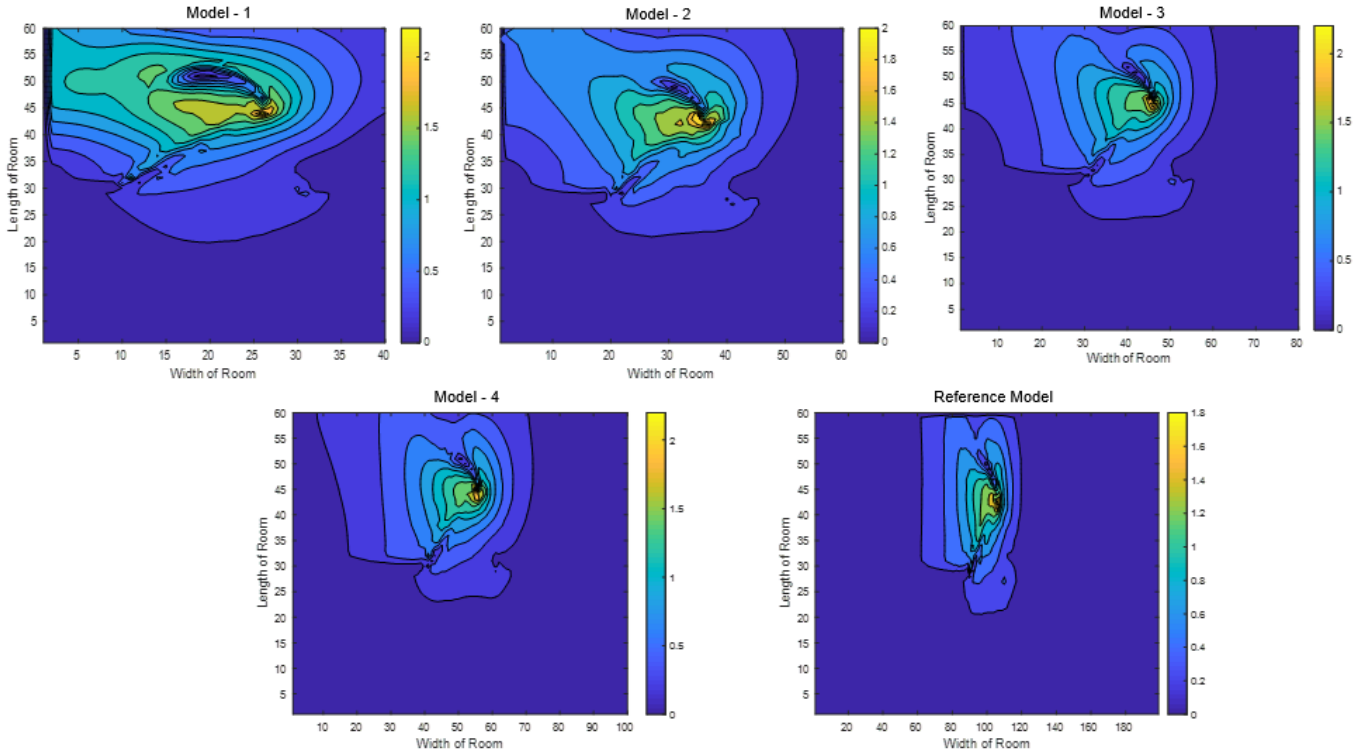

Figure 3. Velocity Distribution and Maximum Velocity when Door was Half-closed

The maximum velocities for each of the model were then identified and the effect of room width defined by the walls were studied. As stated earlier, the largest air speed was associated to the location of door tip. The highest peaks in Graph (a) of Figure 4 for all the models corresponds to the door-tip location. For Model-1, which had a grid width of 40, essentially meaning that the boundaries were pretty close to the region of door movement, the velocity magnitude was highest - 2.36 m/s (7.74 ft/s). Whereas, for Model - 2, 3 and 4 the largest value of velocity magnitude at this point was 2.08 (6.82), 2.21 (7.25) and 2.19 (7.19) m/s (ft/s) respectively and for the reference model, this value was 1.81 m/s (5.94 ft/s). It was understood that as the room width was increasing, there was a declining trend in the largest value of velocity magnitude. This signified that the interference of boundaries with the velocity profiles imparted turbulence which contributed to the increased velocity. It was also noteworthy that with shorter width, the rise to the peak was not smooth whereas, with increasing width, the rise was smooth, for example the reference model. Additionally, after reaching the peak, the velocities near walls were non-zero for narrow models, which was also affecting the relative velocity. But with increasing width and less interference from the boundaries, the near-wall velocity approached zero.

The maximum velocity along the length of the models were also examined and it confirms that the highest speed corresponds to the region surrounded by the door tip. Also, as this was during door closing, velocity was recorded at the outer compartment, the portion below x=30 in Graph (b) of Figure 4, which was around 0.35 m/s (1.15 ft/s) for all the models. A fascinating observation from this figure was the immediate dip in the velocity along the plane where the highest magnitude is observed. The change in speed of air within short space is tabulated in Table 4. For Model 1,

within three grid space along x-axis, the velocity dropped from 2.36 to 0.55 m/s (7.74 to 1.80 ft/s). For Model 2, within same grade space, the speed declined 1.51 in magnitude to 0.57 m/s (6.82 to 1.87 ft/s). For Models - 3 and 4, within two grid spaces, speed dropped 1.64 magnitude points to 0.53 m/s and 0.55 m/s respectively. But, the drop in magnitude for the reference model was 1 magnitude point in terms of m/s and it spanned across 5 grid spaces. Corresponding change in terms of ft/s for models 3, 4, and 5 can be found from Table 4. This fluctuation showed a declining trend with the increase in model width and was the least for the reference model - signifying that boundaries played an important role. This can also be visualized in Figure 3.

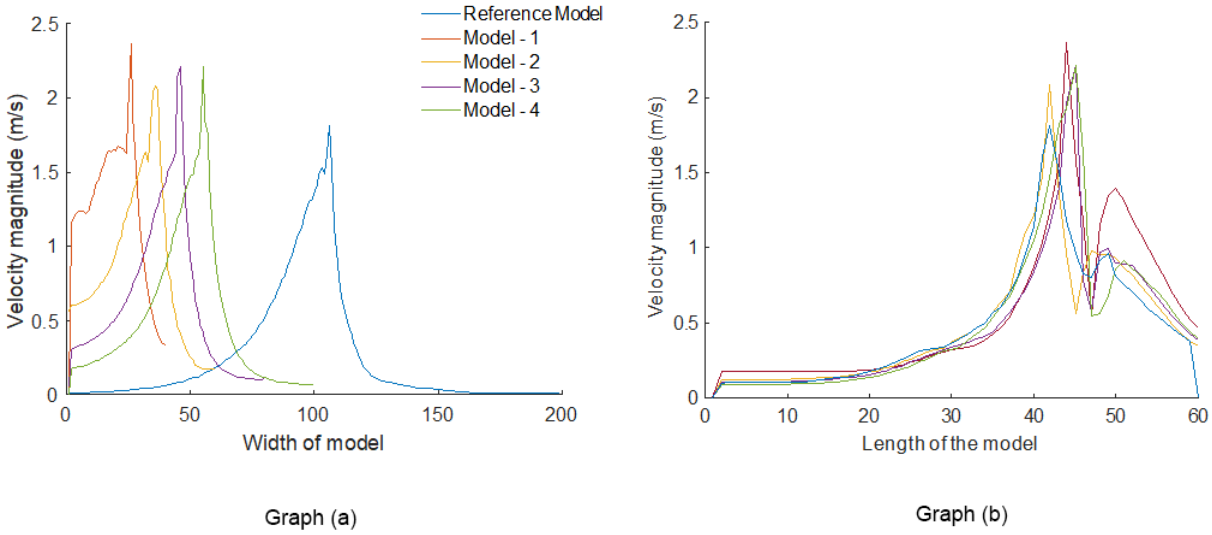

Figure 4. Effect of Model Width and Length on Maximum Velocity

Table 4. The change in Velocity along the length at the plane of maximum magnitude

Model No.	High magnitude of Velocity in m/s (ft/s)	x-coordinate of high magnitude	Low Magnitude of Velocity in m/s (ft/s)	x-coordinate of low magnitude
Model – 1	2.36 (7.74)	44	0.55 (1.80)	47
Model – 2	2.08 (6.82)	42	0.57 (1.87)	45
Model – 3	2.21 (7.25)	45	0.53 (1.74)	47
Model – 4	2.19 (7.19)	45	0.55 (1.80)	47
Reference Model	1.81 (5.94)	42	0.81 (2.66)	47

While looking at the velocity gradients, the maximum gradients were observed near the door wall - as it was constrained with no-slip boundary condition and adjacent to the surface there are velocities - which at some points tends towards the maximum value. For narrower models, the gradient at the right walls were found to be significantly higher than the reference model.

CONCLUSION

In this numerical study, the changes in air velocity with respect to door movement and location of boundaries were examined. This study suggests that the impacts of door closing are more profound on the air movement when compared to the opening motion. The magnitude of air velocity rises sharply during closing motion, as this is essentially reversing the opening motion and the turbulence generated by this contributes to the increase in velocity.

Moreover, narrower the boundaries, sharper is the change in air velocities. Limited availability of space for propagation of wakes generated during door movement facilitates the increase in fluctuation of velocity magnitudes. At the stationary boundary walls as well as the door wall, where velocity was zero, higher velocity gradients were present and for models with tighter spaces, the changes in gradients were sharper, also aiding in increase of speed.

In this study, no complicated inlet and exhaust conditions were simulated. Examining those initial conditions coupled with different types of door motion and effects of boundary geometry are provisions for future studies. This study suggests that this phenomena of the magnitude of velocity rising to the highest value and declining to near-zero close to walls are relatively similar for all the models and one model could be used in order to predict other models, which is an interesting topic for subsequent work.

ACKNOWLEDGEMENT

This work was funded by the NSF-EPSCoR program under Grant # 2012827. The authors are grateful for the support.

REFERENCES

Chen, Q. 1995. "COMPARISON OF DIFFERENT K-ε MODELS FOR INDOOR." *Numerical Heat Transfer, Part B Fundamentals* 28:3:353–69.

Gustavsson N. 2010. "Dispersion of Small Particles into Operating Rooms Due to Openings." CHALMERS UNIVERSITY OF TECHNOLOGY Göteborg,.

J Tu, GH Yeoh, C. Liu. 2018. *Computational Fluid Dynamics: A Practical Approach*. Butterworth-Heinemann an imprint of Elsavier.

Mousavi, Ehsan S. and Kevin R. Grosskopf. 2016. "Airflow Patterns Due to Door Motion and Pressurization in Hospital Isolation Rooms." *Science and Technology for the Built Environment* 22(4):379–84.

Rouaud, Olivier and Michel Havet. 2002. "Computation of the Airflow in a Pilot Scale Clean Room Using K-ε Turbulence Models." *International Journal of Refrigeration* 25(3):351–61.

Sekhar, S. C. and H. C. Willem. 2004. "Impact of Airflow Profile on Indoor Air Quality - a Tropical Study." *Building and Environment* 39(3):255–66.

Smith, Eric B., Ibrahim J. Raphael, Mitchell G. Maltenfort, Sittisak Honsawek, Kyle Dolan, and Elizabeth A. Younkins. 2013. "The Effect of Laminar Air Flow and Door Openings on Operating Room Contamination." *Journal of Arthroplasty* 28(9):1482–85.

Stone, Patricia W. 2009. "Economic Burden of Healthcare-Associated Infections: An American Perspective." *Expert Review of Pharmacoeconomics & Outcomes Research* 9(5):417–22.

Tang, Julian W., I. Eames, Y. Li, Y. A. Taha, P. Wilson, G. Bellingan, K. N. Ward, and J. Breuer. 2005. "Door-Opening Motion Can Potentially Lead to a Transient Breakdown in Negative-Pressure Isolation Conditions: The Importance of Vorticity and Buoyancy Airflows." *Journal of Hospital Infection* 61(4):283–86.